ELSEVIER

International Journal of Heat and Fluid Flow 19 (1998) 439–445

International Journal of
HEAT AND
FLUID FLOW

Exploiting the flexibility of unstructured grids for computing complex flow patterns more precisely

C.-H. Rexroth *, D. Giebert, R. Koch, S. Wittig

Lehrstuhl und Institut für Thermische Strömungsmaschinen, Universität Karlsruhe (TH), D-76128 Karlsruhe, Germany

Abstract

In comparison to structured meshes, the most important advantage of unstructured grids is geometrical flexibility provided by the lack of strict topological rules. The present work proposes techniques to exploit this feature by generating and optimizing unstructured meshes to achieve more accurate results in less computing time. In this article a suited layout of initial grids is shown to improve convergence speed while reducing memory requirements and preserving numerical accuracy. To control the process of solution adaptive grid optimization, normalized gradients of transport variables are proposed. These quantities prove to be effective in several test cases and a demanding turbomachinery application. Although the calculations were carried out assuming two-dimensional flow, the methods introduced here can be applied under three-dimensional conditions without difficulty.

Keywords: Navier-Stokes; SIMPLE(C); Unstructured grid; Mesh refinement/coarsening; Adaption criteria; Test cases

1. Introduction

In the design process of modern gas turbines, numerical methods for the simulation of flow problems are indispensable tools. Because of the complex geometries of relevant parts and components, there is a growing tendency to use unstructured grids instead of their structured predecessors. Unfortunately, this choice is often accompanied by losses in precision and computational efficiency, largely caused by the introduction of triangles or tetrahedra relieving quadrilateral and hexahedral mesh elements. As a result numerical diffusion is usually amplified while the grid topology gets far more complex. However, the unmatched flexibility of unstructured meshes offers the chance to temper or even overcome these drawbacks. In this context the benefits of suited grid design and solution adaptive optimization are discussed in the following.

2. Spatial discretization

It is well known that triangles are suited to cover two-dimensional domains of arbitrary shape without any difficulty. For the Finite Volume procedure used here, the vertices of the triangles serve as nodes of the computational grid. Applying a collocated approach, all transport variables are calculated and stored at these locations. With a Finite Volume method, it is necessary to construct control volumes containing the nodes. A second mesh is derived from the triangulation to define these volumes.

Fig. 1 shows the formation of the dual mesh inside and at the boundaries of a domain. The inner cells are constructed by connecting the centres of all triangles meeting at a node. It should be noticed that these centres are not used to store any flow quantity during the numerical process.

Along the borders of the grid one layer of triangles is skipped to build mesh elements attached to boundary faces. This choice allows for a straightforward implementation of the various boundary conditions.

Differing from bare triangles with only three direct neighbours, the resulting polygonal Finite Volume mesh assures a stronger coupling of the transport variables in adjacent control volumes. Through shared faces each node is in direct contact with all neighbouring cells via convective and diffusive exchange.

3. Numerical algorithm

In continuing earlier work (Noll and Wittig, 1991; Kurreck and Wittig, 1994), a Navier–Stokes code using the Finite Volume method on two-dimensional unstructured grids has been developed to meet the requirements arising from flow problems in turbomachinery (Rexroth and Wittig, 1995).

The governing transport equations are solved in a blockiterative manner. The velocity field is derived from Reynolds-averaged Navier–Stokes equations. A pressure distribution is calculated by a SIMPLE(C)-type correction algorithm (Patankar, 1981; Van Doormaal and Raithby, 1984) where a special interpolation of cell face velocities (Rhie and Chow, 1983)

* Corresponding author. Address: Dieburger Strasse 238a, D-64287 Darmstadt, Germany. E-mail: chr@fluent.de.

0142-727X/98/$ – see front matter
PII: S0142-727X(98)10014-0

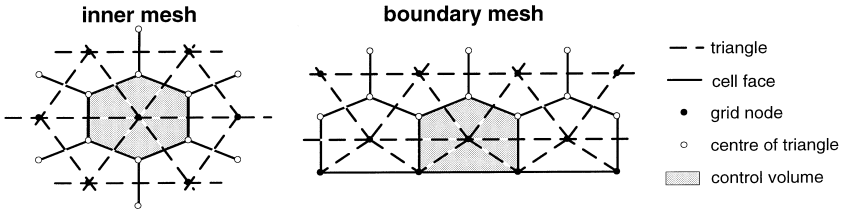

Fig. 1. Topology of control volumes (duals).

prevents chess-board oscillations on the collocated grid. An extension for the treatment of compressibility has also been implemented (Karki and Patankar, 1989). Turbulent quantities are calculated by applying the standard k,ϵ model together with a logarithmic wall function (Launder and Spalding, 1974). A transport equation for the enthalpy accounts for an exchange of energy. To assure second order accurate, bounded and stable modelling of the convective terms, a new Derivative based Interpolation Scheme for Convection (DISC) is available (Rexroth et al., 1997). Differing from approaches developed on structured grids, DISC just requires local information on flow quantities, to determine their cell face values. That way time consuming search for upstream data points is avoided.

To assure a fast implicit solution of the linear equations the iterative BiCGSTAB algorithm (Van der Vorst, 1992) combined with a reduced ILU decomposition is applied. It rarely takes more than one iteration of BiCGSTAB to reduce the residual of a linear system for a single transport variable by more than two orders of magnitude.

For enhancement of overall reliability and efficiency of the flow solver, certain acceleration techniques developed recently have been introduced (Rexroth and Wittig, 1997).

4. Exploiting geometrical flexibility

Already at the stage of grid generation, it is possible to profit from the geometrical flexibility of unstructured meshes. Based on a rough estimation, the spatial resolution of a grid can be chosen conformable to the mean flow pattern. A related strategy is the acceleration of convergence (AC) by a special grid design. Finally, existing meshes can be optimized by adapting the grid density to the character of the calculated flow field. The pay off is a significant gain in accuracy, if the basic grid is relatively coarse. Both methods are capable to reduce memory and time requirements.

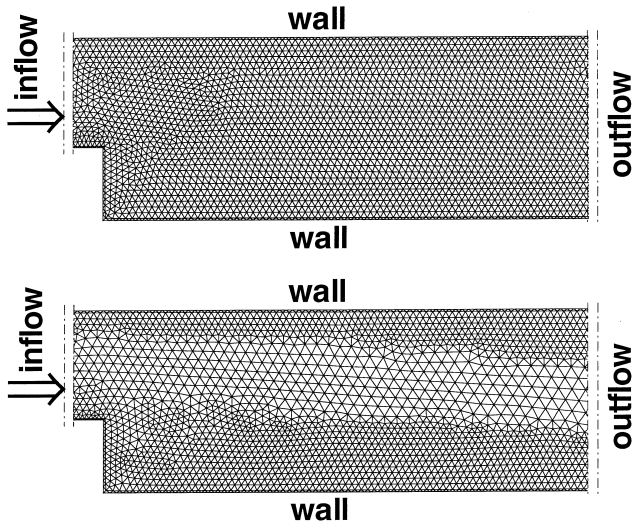

Fig. 2. Conventional grid and AC grid for step flow.

4.1. Grid generation

Fig. 2 presents two different grids for the common test case of a turbulent flow over a backward facing step (Eaton and Johnston, 1980).

On top, there is a section of a conventional mesh with uniform spatial resolution, consisting of 9695 nodes. The second grid takes advantage of the assumption, that near the centre line of the domain no steep gradients in flow quantities will be found. By prescribing a coarser resolution in this region, the number of grid nodes can be reduced to 6924 without loss of information inside the boundary layers.

As an additional effect, the number of mesh cells the flow has to cross on its way from inflow to outflow boundary is re-

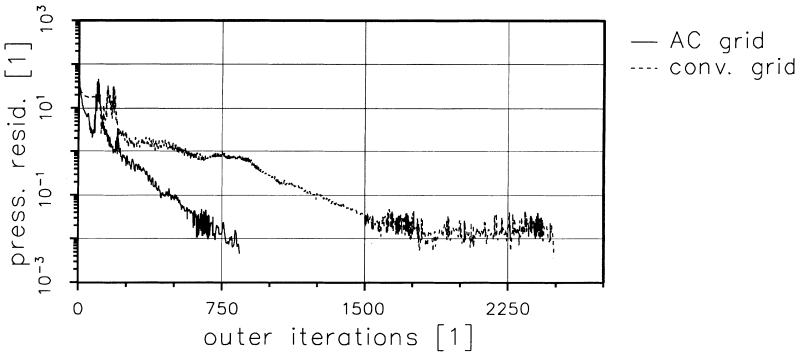

Fig. 3. Convergence of step flow calculations.

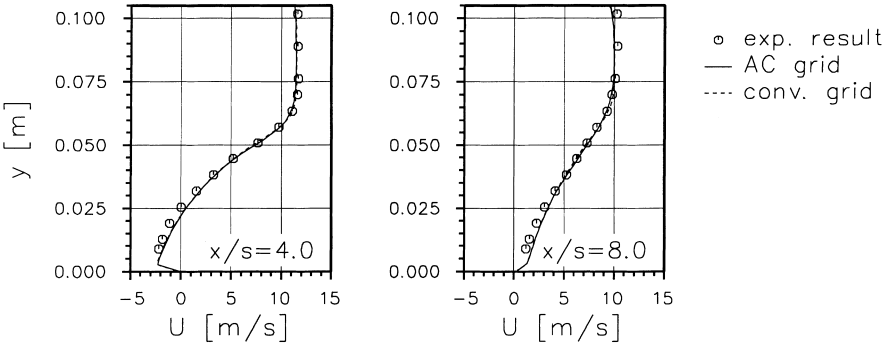

Fig. 4. Velocity profiles for step flow.

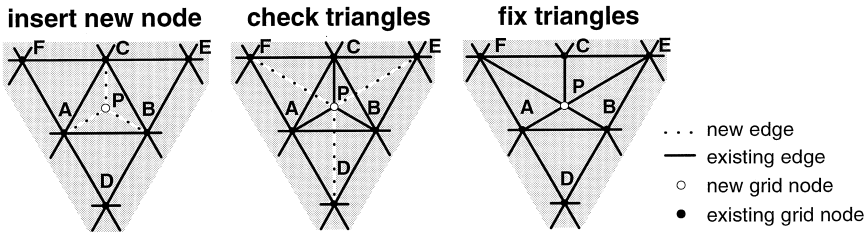

Fig. 5. Adding new grid nodes.

duced in the coarse grid area. Therefore, information passes much easier, enhancing the coupling between distant parts of the domain. Consequently, as a main advantage, convergence is accelerated (AC).

The corresponding convergence history in terms of normalized pressure residual (Res) and number of outer iterations can be found in Fig. 3. Here the pressure residual is defined as the maximum difference between pressure solutions of successive blockiterations, divided by the incoming mass flow.

On the conventional grid 2490 blockiterations and 165.5 min of computing time on a Sun Sparc 10-TGX4 workstation are required to achieve the stopping criterion of $\mathrm{Res} \leqslant 5 \cdot 10^{-3}$ for the blockiteration. With the AC grid, the same procedure is finished after 842 loops and 33.6 min.

Close to the convergence limit, the pressure residuals start to oscillate in both cases. This can be attributed to the convergence criterion chosen for the BiCGSTAB algorithm solving the arising linear systems of equations. It has been set to the same value as the outer stopping criterion. Therefore near convergence the gain in accuracy achieved during one outer iteration is getting smaller.

In Fig. 4, numerical and experimental results for the axial component U of the velocity are compared at two positions located 4.0 and 8.0 step heights s downstream of the expansion. In spite of reducing the numerical effort to 20%, the AC grid arrives at almost exactly the same results as the conventional approach. Due to the turbulence model applied, the length of the separation zone is underestimated.

In cases, where a comparison with measurements is not possible, the response of the AC solution to successive refinement and optimization of the grid should be monitored carefully.

4.2. Grid optimization

To modify the spatial resolution of a mesh, grid nodes can be added or removed. The methods used are designed to preserve the connectivity of existing nodes as far as possible.

As can be seen from Fig. 5, a new node P is inserted at the centre of the triangle ABC, thereby divided into three smaller triangles. To reduce distortions in the vicinity of the new node, the altered mesh has to be checked and optimized. Therefore the edges AB, BC and CA are swapped, whenever the minimum angle in the alternative triangulation will be higher than in the present state. In Fig. 5 the edges BC and CA have been swapped for demonstration without looking at the exact geometric criteria. Afterwards the new topology is fixed.

The technique to delete grid nodes is shown in Fig. 6. In the first step a new node P is inserted at the centre of an existing triangle, too. Then its three neighbours are deleted and P is connected to all surrounding nodes. The new edges are checked and swapped according to the rules explained before. Again in Fig. 6 some connections have been changed just for demonstration. What remains to be done is fixing the triangles. Both procedures end with a smoothing of the modified mesh.

A grid can be optimized either under complete control of the user or automatically in a programmed algorithm. In each case various options are at hand. For an automatic adaption to the pattern of a calculated flow field, non-dimensional gradients $P(\phi_i)$ of the transport variables ϕ_i are used.

$$P(\phi_i) = \left[\left|\frac{\partial \phi_i}{\partial x}\right| + \left|\frac{\partial \phi_i}{\partial y}\right|\right] \cdot \frac{D}{|\phi_{i,\mathrm{ref}}|} \tag{1}$$

$P(\phi_i)$ is evaluated at the grid nodes from spatial derivatives $\partial\phi_i/\partial x_j$ of flow quantities, the mean diameter D and a reference value $\phi_{i,\mathrm{ref}}$ at the corresponding mesh cell.

The expressions $\partial\phi_i/\partial x_j \cdot D$ may be interpreted as first order terms of a Taylor expansion for an unknown ϕ_i. At locations, where the grid density is insufficient, strong variations of ϕ_i are associated with high values of $P(\phi_i)$. In these areas, there is an enlarged probability of numerical inaccuracies. Therefore, $P(\phi_i)$ can be regarded as an indicator for the local discretization error of ϕ_i. For high values of $P(\phi_i)$ grid refinement is required, whereas low values permit coarsening.

An advantage of the formulation proposed for the error estimator $P(\phi_i)$ is the possibility of minimization. With refined spatial resolution the cell diameters D become smaller, leading to reduced values of $P(\phi_i)$. Normalization by $\phi_{i,\mathrm{ref}}$ takes into account the absolute local magnitude of a transport variable.

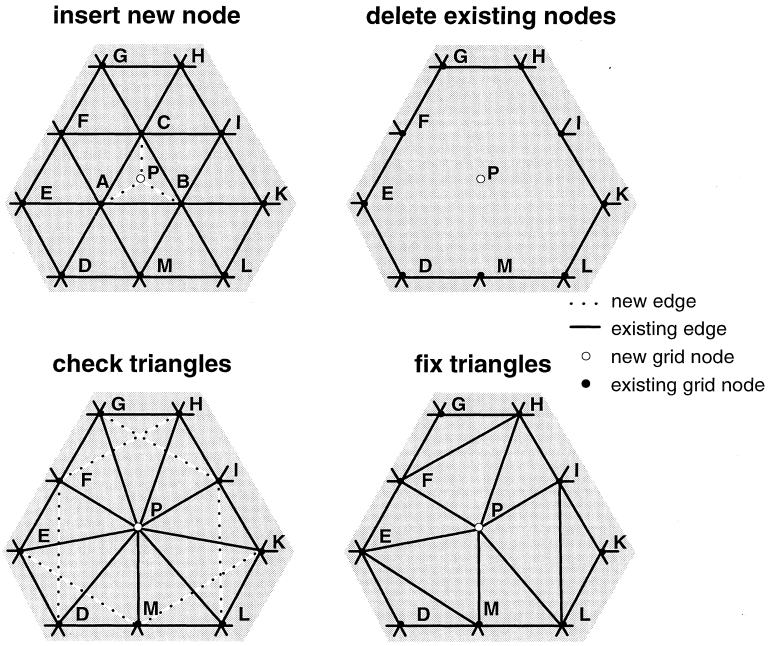

Fig. 6. Removing existing grid nodes.

Fig. 7 illustrates the distribution of $P(u,v)(=P(u)+P(v))$ on the basic AC grid as well as the adapted mesh for the backward facing step.

Refinement was performed downstream of the expansion where flow separation provokes a high level of $P(u,v)$. On the optimized grid almost constant values of $P(u,v)$ were found. Besides zones of detached flow, $P(u,v)$ is also sensitive to boundary layers and stagnation points.

In transonic flows, the grid optimization procedure can be applied for shock capturing. As an example, the basic grid and evaluations of different adaption parameters $P(\phi_i)$ are shown in Fig. 8 for a transonic channel flow (Liu and Squire, 1988).

Over a circular arc at the bottom wall of the channel, the flow accelerates to transonic speed. Near the trailing edge of the profile a Mach number of 1.27 is attained, before recompression takes place. As can be seen from Fig. 8 without difficulties, $P(u,v)$ and $P(p)$ are able to locate the shock, but the product $P(u,v)\cdot P(p)$ of both quantities leads to contours which are confined even better.

Fig. 9 presents the same mesh after optimization based on the former criterion. The position of the shock itself and an

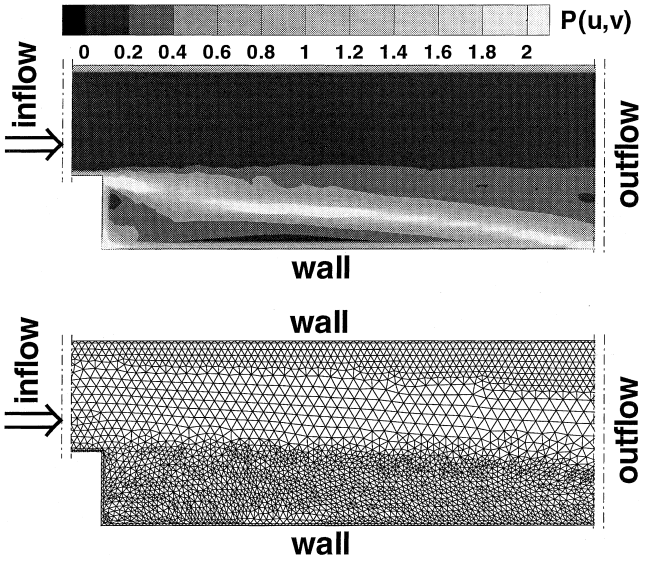

Fig. 7. $P(u,v)$ and modified AC grid.

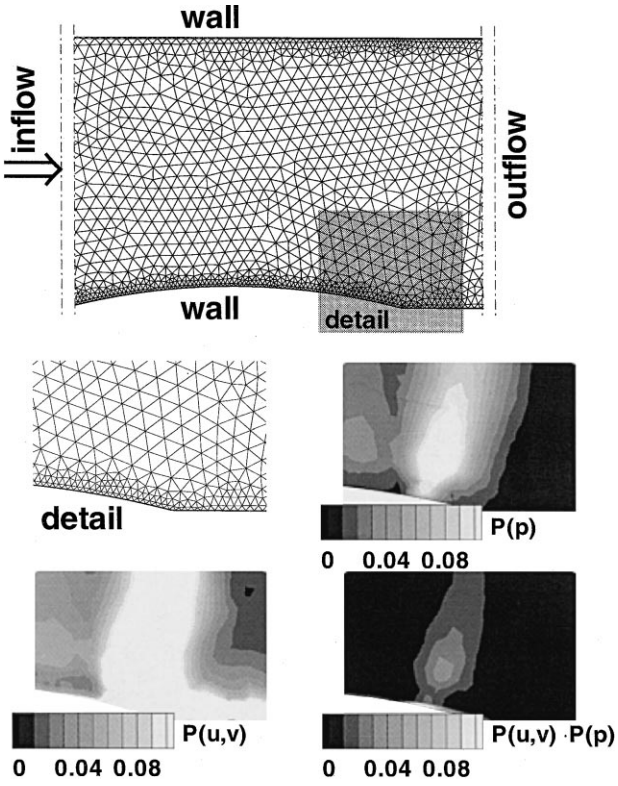

Fig. 8. Basic grid and $P(\phi_i)$ for channel flow.

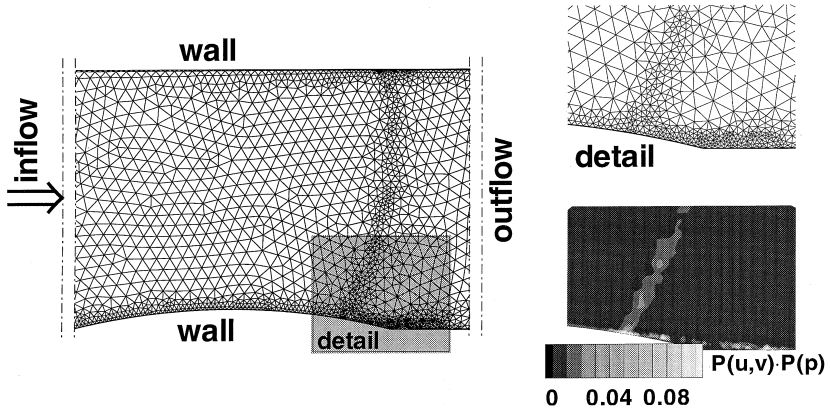

Fig. 9. Modif. grid and $P(u,v)\cdot P(p)$ for channel flow.

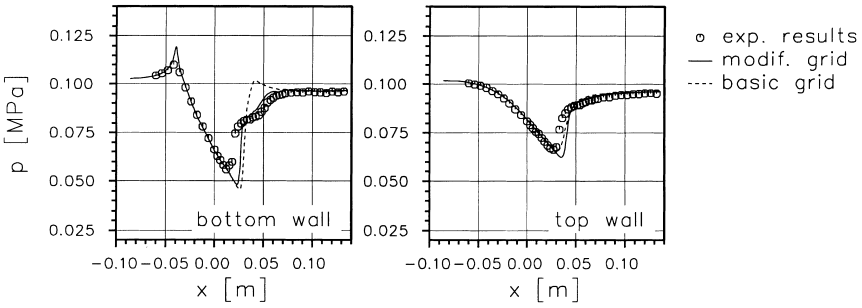

Fig. 10. Wall pressure for channel flow.

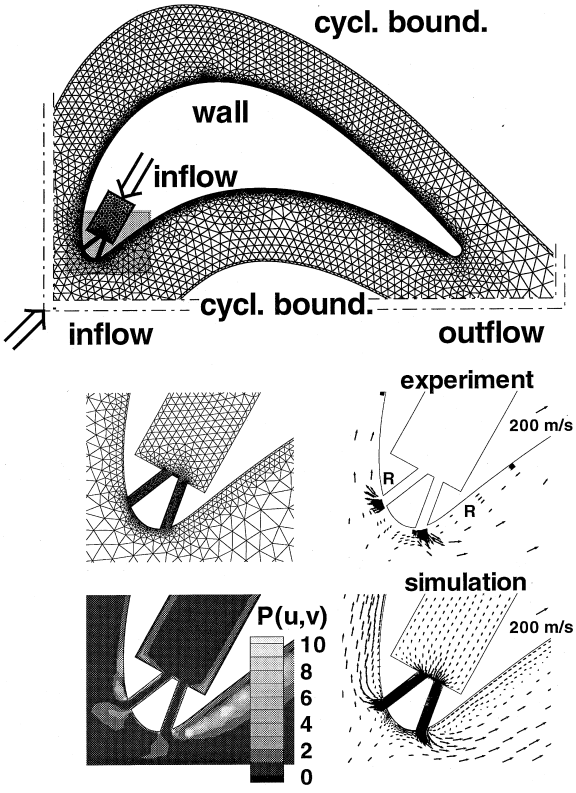

Fig. 11. Basic grid, velocity and $P(u,v)$ at LE for cascade.

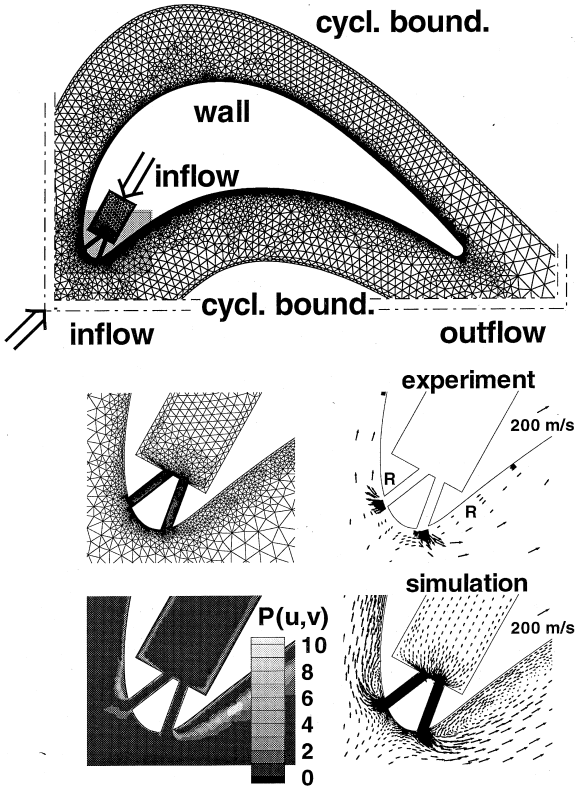

Fig. 12. Modif. grid, velocity and $P(u,v)$ at LE for cascade.

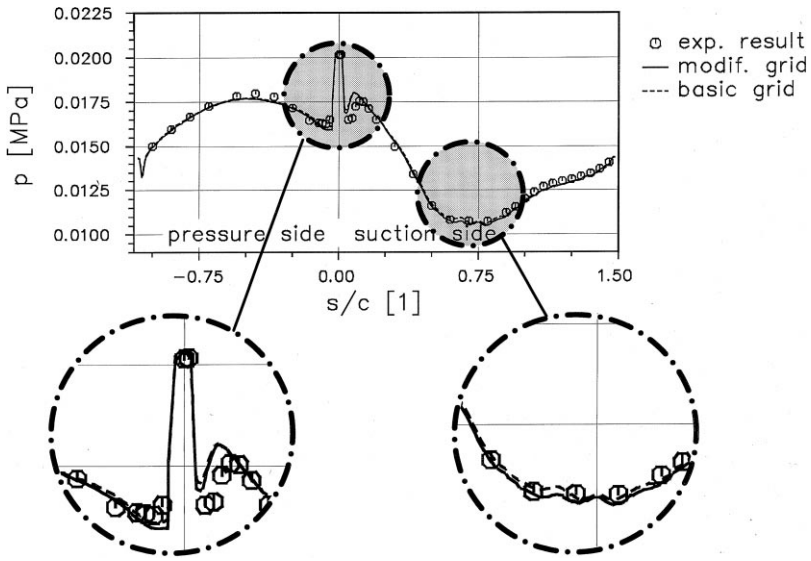

Fig. 13. Wall pressure for filmcooled cascade.

induced flow separation near the bottom wall are clearly visible from grid resolution. The area, where peak values of the optimization parameter $P(u,v)\cdot P(p)$ can be found, has also been reduced significantly.

To demonstrate the improvement of accuracy gained by the refinement, Fig. 10 shows a comparison of the pressure distributions calculated along the top and the bottom wall with experimental findings.

On the modified grid, the shock has moved a little further downstream at the top of the channel. Despite the simple wall function approach used to bridge the boundary layer, the delay in pressure recovery caused by the flow separation at the trailing edge of the arc, which has been suppressed on the coarser grid, can be resolved to a certain extent now.

5. Practical application

Another example of grid optimization is given in Fig. 11.

For this practical application the flow through a cascade of film cooled gas turbine blades has been selected (Beeck et al., 1992). The basic mesh is made up by 5787 grid nodes. It consists of the outer domain, the two cooling air channels opening near the leading edge of the blade (LE) and a plenum where the cooling flow is supplied.

Experiments were carried out at a blowing ration $M=(\rho|\vec{w}|)_{\text{cool}}/(\rho|\vec{w}|)_{\infty}$ of 1.14. Downstream of both cooling air injections, large separation bubbles have been found. These characteristic features of the flow field are already present in the simulation on the basic grid. With the help of the optimization parameter $P(u,v)$ critical mesh areas could be identified in front of the cooling jets and inside the recirculation zones next to them. Adaption also takes place in the surface boundary layer and inside the wake following the trailing edge of the blade.

Evaluating $P(u,v)$, the mesh was refined by 2262 additional nodes. Fig. 12 shows, how the spatial resolution has been optimized, especially in the vicinity of the leading edge of the profile (LE). Therefore, the structure of flow separation is predicted in detail. According to the new contours of $P(u,v)$ the extension of critical areas in the flow field has been reduced, too.

For a quantitative rating of accuracy, Fig. 13 presents measured and calculated profiles of the pressure along the surface of the blade. The surface coordinate s has been normalized by the chord length c. Results from basic and modified grid are in very good agreement with the measurements. The adapted mesh improves accuracy inside both separation zones and near the pressure minimum on the suction side.

6. Conclusion

The geometrical flexibility of unstructured grids can be exploited to enhance accuracy and reduce computing time of numerical flow calculations.

Time requirements are cut down by prescribing a spatial resolution of the initial mesh that is capable to accelerate convergence by improving the exchange of information inside the domain.

A gain in accuracy is attained by adapting the grid to the character of the simulated flow field. The optimization criteria presented in this paper are suited to identify critical zones inside a domain, e.g. flow separations, shocks, stagnation points and boundary layers.

Acknowledgements

This work was supported by a grant of the Deutsche Forschungsgemeinschaft in the context of the Graduiertenkolleg 'Energie- und Umwelttechnik' and the Sonderforschungsbereich 167 'Hochbelastete Brennräume'.

References

Beeck, A., Fottner, L., Benz, E., Wittig, S., 1992. The aerodynamic effect of coolant ejection in the leading edge region of a film-cooled turbine blade. In: Proceedings of 80th International Symposium on Heat Transfer and Cooling in Gas Turbines, Antalya, Turkey.

Eaton, J.K., Johnston, J.P., 1980. Turbulent flow reattachment: An experimental study of the flow and structure behind a backward facing step. Stanford University Department of Mechanical Engineering, Report MD-39.

Karki, K.C., Patankar, S.V., 1989. Pressure based calculation procedure for viscous flows at all speeds in arbitrary configurations. AIAA Journal 27, 1167–1174.

Kurreck, M., Wittig, S., 1994. Numerical simulation of combustor flows on parallel computers: Potential limitations and practical experience. ASME Paper 94-GT-404.

Launder, B.E., Spalding, D.B., 1974. The numerical computation of turbulent flows. Computer Methods in Applied Mechanics and Engineering 3, 269–289.

Liu, X., Squire, L.C., 1988. An investigation of shock/boundary-layer interactions on curved surfaces at transonic speeds. Journal of Fluid Mechanics 187, 67–486.

Noll, B.E., Wittig, S., 1991. A generalized conjugate gradient method for the efficient solution of three-dimensional fluid flow problems. Numerical Heat Transfer 20, 207–221.

Patankar, S.V., 1981. A calculation procedure for two-dimensional elliptic situations. Numerical Heat Transfer 4, 409–425.

Rexroth, C.-H., Wittig, S., 1995. Improved accuracy and effectiveness for Navier-Stokes solvers on unstructured grids. In: Numerical Methods for Fluid Dynamics V, Oxford Science Publications, London, pp. 549–556.

Rexroth, C.-H., Bauer, H.-J., Wittig, S., 1997. DISC-An efficient method for the discretization of convection on unstructured grids. Aerospace Science and Technology 1 (6).

Rexroth, C.-H., Wittig, S., 1997. Techniques to enhance reliability and efficiency of flow calculations on unstructured grids. Notes on Numerical Fluid Mechanics 60, 275–282.

Rhie, C.M., Chow, W.L., 1983. Numerical study of the turbulent flow past an airfoil with trailing edge separation. AIAA Journal 21, 1525–1532.

Van der Vorst, H.A., 1992. Bi-CGSTAB: A fast and smoothly converging variant of Bi-CG for the solution of nonsymmetric linear systems. SIAM Journal on Scientific and Statistical Computing 13, 631–644.

Van Doormaal, J.P., Raithby, G.D., 1984. Enhancement of the SIMPLE method for predicting incompressible fluid flows. Numerical Heat Transfer 7, 147–163.